Analysis of fracture initiation pressure of horizontal well in transversely isotropic shale reservoirs

Lichun Jia, Hu Deng, Dianchen Liu, Zhilin Li, Weicheng Li
Drilling & Production Technology Research Institute of CNPC Chuanqing Drilling Engineering Company Limited, Guanghan, PR China

ABSTRACT: This study aims at analyzing the fracture initiation pressure (FIP) of horizontal wellbore in anisotropic shale by considering elastic and strength anisotropy. The FIP is deduced as a function of the anisotropic elastic properties, in-situ stresses, anisotropic tensile strength as well as bedding dip. The results show that the increase of the anisotropy of Young's modulus, Poisson′s ratio and horizontal in-situ stress induces a reduction of the FIP. While an increase of tensile strength ratio T_v/T_h and bedding dip will increase the FIP. It is concluded that the influence of E_h/E_v on FIP is the highest, followed by σ_H/σ_h, and then T_v/T_h, while the influence of Poisson's ratio is the lowest. For the effect of azimuth of horizontal well, the FIP increases first and then decreases when the horizontal borehole azimuth is far away from the direction of maximum horizontal stress.

Keywords: shale, transversely isotropic, fracture initiation pressure, modulus anisotropy, Poisson's ratio anisotropy, tensile strength anisotropy.

1 INTRODUCTION

Borehole fracture initiation occurs when the stress at borehole wall exceeds the tensile strength during drilling or hydraulic fracturing (Guo et al. 1992 and Ong & Roegiers 1995). The tensile failure of formation would induce lost circulation during drilling, which is a most costly problem in increasing the non-productive time (Ma et al. 2017). The wellbore pressure which initiates new fractures is known as fracture initiation pressure (FIP). In theory, the FIP can be calculated as the stress distribution around the wellbore and the tensile strength criterion of the formation are known (Ma et al. 2019). In a homogenous isotropic formation, the Hubbert-Willis model, Matthews-Kelly model, Haimson-Fairhurst model are commonly used models in calculation of FIP (Zhang & Yin 2017 and Sampath et al. 2018). However, the above models could cause errors as used in prediction of FIP in sedimentary rocks, which show distinct anisotropy in mechanical behaviors (Ma et al. 2022). Shale, as a typical sedimentary rock, shows inherently anisotropic behaviour due to the bedding planes and laminations (Li & Jia 2018). The horizontal drilling and multistage hydraulic fracturing play an important role in commercial development of shale gas. Reducing lost circulation for safe drilling and improving hydraulic fracturing operation, both demand an accuracy calculation of FIP.

Much work has been done in the wellbore stability analysis of anisotropic formations (Gupta & Zaman 1999 and Zhao et al. 2018). Aadnoy (1989) used the anisotropic body theory to propose wellbore stability model, but only considering the anisotropic modulus and shear strength. Ong & Roegiers (1995) investigated the fracture initiation from inclined wellbores in anisotropic formations. However, these models just considered the influence of rock anisotropy, such as anisotropy of horizontal and vertical Young's modulus, on the fracture initiation pressure, which ignored the anisotropy of tensile strength due to the existence of bedding planes. To improve prediction accuracy of FIP, Ma et al. (2019 & 2022) studied the influence of both elastic anisotropy and strength anisotropy by using four typical tensile failure criteria and the Nova-Zaninetti (N-Z) criterion is recommended for transversely isotropic shale. Do et al. (2017) assessed both effects of hydraulic and mechanical anisotropy on the FIP in permeable rocks. But there are still rare in considering both rock anisotropy and tensile strength anisotropy for FIP of horizontal wells in shale. Therefore, this study is to investigate the FIP of horizontal well in transversely isotropic shale with considering both elastic parameters anisotropy and tensile strength anisotropy. And the factors influencing the fracture initiation pressure, such as anisotropic elastic properties, the in-situ stresses, anisotropic tensile strength as well as bedding dip angle, are analyzed in detail. Finally, the cloture of this work is conducted with some conclusions.

2 FRACTURE INITIATION PRESSURE FOR TRANSVERSELY ISOTROPIC ROCKS

2.1 Stress distribution on borehole wall

For transversely isotropic formation, the stress distribution around a circular borehole with a generalized plane strain state is given by (Ong & Roegiers 1995, Gupta & Zaman 1999):

$$\begin{cases} \sigma_{xx} = \sigma_{xx}^b + \sigma_{xx,h} = \sigma_{xx}^b + 2Re[\mu_1^2\phi_1'(z_1) + \mu_2^2\phi_2'(z_2) + \lambda_3\mu_3^2\phi_3'(z_3)] \\ \sigma_{yy} = \sigma_{yy}^b + \sigma_{yy,h} = \sigma_{yy}^b + 2Re[\phi_1'(z_1) + \phi_2'(z_2) + \lambda_3\phi_3'(z_3)] \\ \tau_{xy} = \tau_{xy}^b + \tau_{xy,h} = \tau_{xy}^b - 2Re[\mu_1\phi_1'(z_1) + \mu_2\phi_2'(z_2) + \lambda_3\mu_3\phi_3'(z_3)] \\ \tau_{xz} = \tau_{xz}^b + \tau_{xz,h} = \tau_{xz}^b + 2Re[\lambda_1\mu_1\phi_1'(z_1) + \lambda_2\mu_2\phi_2'(z_2) + \mu_3\phi_3'(z_3)] \\ \tau_{yz} = \tau_{yz}^b + \tau_{yz,h} = \tau_{yz}^b - 2Re[\lambda_1\phi_1'(z_1) + \lambda_2\phi_2'(z_2) + \phi_3'(z_3)] \\ \sigma_{zz} = \sigma_{zz}^b - \dfrac{1}{a_{33}}\left[a_{31}\sigma_{xx,h} + a_{32}\sigma_{yy,h} + a_{34}\tau_{yz,h} + a_{35}\tau_{xz,h} + a_{36}\tau_{xy,h}\right] \end{cases} \quad (1)$$

where σ_{xx}, σ_{yy}, σ_{zz}, τ_{xy}, τ_{xz} and τ_{yz} are the stress components around the wellbore in a rectangular coordinate system, MPa; σ_{xx}^b, σ_{yy}^b, σ_{zz}^b, τ_{xy}^b, τ_{xz}^b, and τ_{yz}^b are far field stresses, MPa; *Re* is the notation for the real part of the complex expressions in the brackets; $\phi_k'(z_k)$ (k=1, 2, 3) is the analytic function of the complex variable z_k=x+$y\mu_k$, which can be got in the study of Ong & Roegiers (1995); μ_k is the characteristic root of the characteristic equation corresponding to the strain compatibility equation; λ_k is the three complex numbers; a_{31}, a_{32}, a_{33}, a_{34}, a_{35} and a_{36} are the components of the compliance coefficient matrix of transversely isotropic formation, which can be expressed by five independent elastic constants, including two Young's modulus (E_h and E_v), two Poisson's ratio (v_h and v_v) and one shear modulus (G_v).

The far field stress components of horizontal well are expressed as:

$$\begin{cases} \sigma_{xx}^b = \sigma_v \\ \sigma_{yy}^b = \sigma_H \sin^2(\beta - \varphi) + \sigma_h \cos^2(\beta - \varphi) \\ \sigma_{zz}^b = \sigma_H \cos^2(\beta - \varphi) + \sigma_h \sin^2(\beta - \varphi) \\ \tau_{yz}^b = (\sigma_h - \sigma_H)\sin(\beta - \varphi)\cos(\beta - \varphi) \\ \tau_{xy}^b = \tau_{xz}^b = 0 \end{cases} \quad (2)$$

where σ_H and σ_h is the maximum and minimum horizontal stress, respectively, MPa; σ_v is the vertical stress, MPa; β is the azimuth angle of borehole, (°); φ is the azimuth angle of maximum horizontal stress, (°).

The stresses around the wellbore in cylindrical coordinate system are as follows (Li & Jia 2018):

$$\begin{cases} \sigma'_{rr} = p_w \\ \sigma'_{\theta\theta} = \sigma_{xx}\sin^2\theta + \sigma_{yy}\cos^2\theta - \tau_{xy}\sin 2\theta \\ \sigma'_{zz} = \sigma_{zz} \\ \tau'_{r\theta} = \frac{1}{2}(\sigma_{yy} - \sigma_{xx})\sin 2\theta + \tau_{xy}\cos 2\theta \\ \tau'_{\theta z} = \tau'_{rz} = 0 \end{cases} \tag{3}$$

where σ'_{rr}, $\sigma'_{\theta\theta}$ and σ'_{zz} are the radial, tangential and axial stress around wellbore, respectively, MPa; $\tau'_{\theta z}$, τ'_{rz} and $\tau'_{r\theta}$ are shear stresses around wellbore, respectively, MPa; p_w is wellbore fluid pressure, MPa; θ is the circumferential angle on the borehole wall, (°).

2.2 Fracture initiation pressure model

From the stress distribution on borehole wall, three principal stresses are given by (Ma et al. 2022):

$$\begin{cases} \sigma_1 = \sigma'_{rr} \\ \sigma_2 = \dfrac{\sigma'_{\theta\theta} + \sigma'_{zz}}{2} + \dfrac{1}{2}\sqrt{(\sigma'_{\theta\theta} - \sigma'_{zz})^2 + 4(\tau'_{\theta z})^2} \\ \sigma_3 = \dfrac{\sigma'_{\theta\theta} + \sigma'_{zz}}{2} - \dfrac{1}{2}\sqrt{(\sigma'_{\theta\theta} - \sigma'_{zz})^2 + 4(\tau'_{\theta z})^2} \end{cases} \tag{4}$$

where, σ_1, σ_2, σ_3 is the maximum, intermediate and minimum principal stress, respectively, MPa.

According to the minimum normal stress theory, tensile failure of borehole will occur when the effective minimum principal stress reaches the tensile strength of formation. Consequently, the tensile failure criterion of horizontal well can be written as (Ma et al. 2017):

$$\sigma_3 - \alpha p_p + \mathrm{T}(\beta_b) = 0 \tag{5}$$

where, α is the Biot coefficient, dimensionless; β_b is the angle between the tensile stress and bedding normal, (°); p_p is pore pressure, MPa; $T(\beta_b)$ is the tensile strength at a given angle β_b, MPa.

For transversely isotropic shale, the tensile failure criteria, namely Nova-Zaninetti (N-Z) criterion, and Lee-Pietruszczak (L-P) criterion, are more applicable to shale (Ma et al. 2017). Here, the L-P criterion is adopted for calculation of fracture initiation pressure (FIP):

$$\mathrm{T}(\beta_b) = \frac{T_h + T_v}{2} - \frac{T_v - T_h}{2}\cos 2\beta_b \tag{6}$$

where, T_v and T_h are tensile strengths of shale matrix and bedding planes, respectively, MPa.

The angle β_b can be calculated as following (Ma et al. 2022):

$$\beta_b = \cos^{-1}\frac{m_1 n_1 + m_2 n_2 + m_3 n_3}{\sqrt{m_1^2 + m_2^2 + m_3^2}\sqrt{n_1^2 + n_2^2 + n_3^2}} \tag{7}$$

$$\begin{cases} m_1 = \sin\alpha_w \cos\beta_w \\ m_2 = \sin\alpha_w \sin\beta_w \\ m_3 = \cos\alpha_w \end{cases} \tag{8}$$

$$\begin{cases} n_1 = \cos\varphi\cos\gamma - \sin\varphi\cos\theta \\ n_2 = \sin\varphi\cos\gamma + \cos\varphi\cos\theta \\ n_3 = -\sin\theta \end{cases} \tag{9}$$

where, β_w and α_w are the azimuth and dip of bedding plane, respectively, (°); φ is the azimuth angle of maximum horizontal stress, (°); γ is the angle of tensile fracture trace at wellbore wall, which is calculated using (Ong & Roegiers 1995):

$$\gamma = \frac{1}{2}\tan^{-1}\frac{2\tau_{\theta z}}{\sigma_{\theta\theta} - \sigma_{zz}} + \frac{\pi}{2} \tag{10}$$

Finally, the fracture initiation pressure (FIP) is determined as one corresponding to the minimum value of minimum principal stress σ_3 obtained from all circumferential angle θ on the borehole wall.

3 RESULTS AND ANALYSIS OF THE FRACTURE INITIATION PRESSURE

The following basic parameters are used to calculate the FIP of horizontal well in a anisotropic shale reservoir: the vertical in-situ stress σ_v=63.2MPa, the maximum horizontal stress σ_H =75.5MPa, the minimum horizontal stress σ_h=52.6MPa, the pore pressure p_p=48.5MPa, the Biot's coefficient α=0.8, the Young's modulus parallel and perpendicular to bedding E_h=35.87GPa and E_v=29.73GPa, the Poisson's ratio parallel and perpendicular to bedding v_h=0.23 and v_v =0.26, the tensile strength of bedding and shale matrix T_h=5.16MPa and T_v =15.58MPa, the dip and direction of bedding α_w=30° and β_w=30°, the azimuth of borehole and maximum horizontal stress β=0° and φ=0°, respectively.

3.1 Effect of Young's modulus ratio E_h/E_v

The distribution of wellbore pressure necessary to initiate the fracture with circumferential angle on the borehole wall and variation of FIP under different ratio of E_h/E_v are illustrated in Figure 1. Here, E_h=35.87GPa remains constant while E_v changes gradually for obtaining different E_h/E_v. It is clear shown that the Young's modulus anisotropy has a great influence on distribution of wellbore pressure necessary to initiate fracture. And the FIP decreases with the increase of E_h/E_v and the decline rate becomes lower at higher anisotropy. There is a negative correlation between FIP and ratio E_h/E_v. This indicates that the fracture is easy to initiate under a higher anisotropy of Young's modulus in shale.

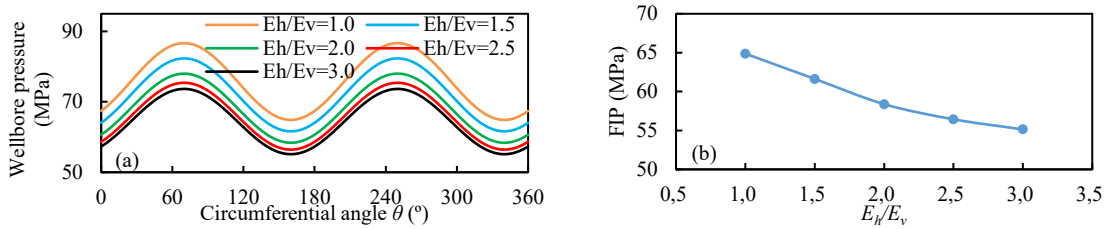

Figure 1. Distribution of wellbore pressure with angle θ (a) and variation of FIP (b) under different E_h/E_v.

3.2 Effect of Poisson's ratio v_h/v_v

Figure 2 shows the distribution of wellbore pressure necessary to initiate the fracture with circumferential angle and variation of FIP under different ratio of v_h/v_v. Similarly, the FIP gradually decreases from 62.21MPa to 60.87MPa as the ratio of v_h/v_v increases, but the reduction range is very small as compared with the influence of ratio E_h/E_v, which indicates that Poisson′s ratio anisotropy has little effect on fracture initiation pressure.

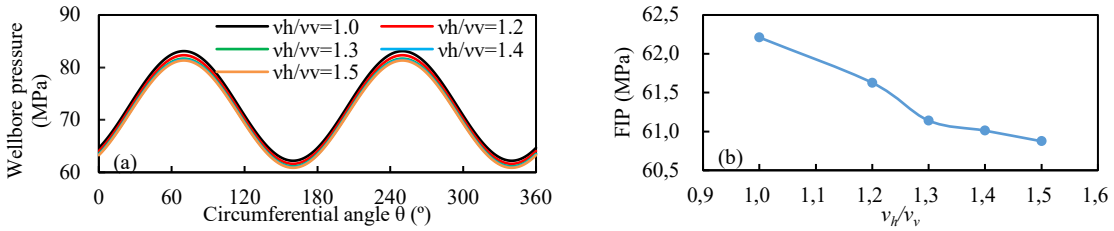

Figure 2. Distribution of wellbore pressure with angle θ (a) and variation of FIP (b) under different v_h/v_v.

3.3 *Effect of tensile strength ratio T_v/T_h*

The effect of tensile strength ratio T_v/T_h on the distribution of wellbore pressure with circumferential angle and variation of FIP are plotted in Figure 3. It is clearly found that with the increase of anisotropy of tensile strength, the FIP shows an obvious increasing trend, which represents an approximately linear relationship with ratio T_v/T_h. The difference between T_v/T_h=3 and T_v/T_h=1 is 5.69MPa while the difference of Young's modulus is 9.73MPa, meaning that the influence of tensile strength anisotropy is slightly lower than that of Young's modulus anisotropy but much higher than that of Poisson′s ratio.

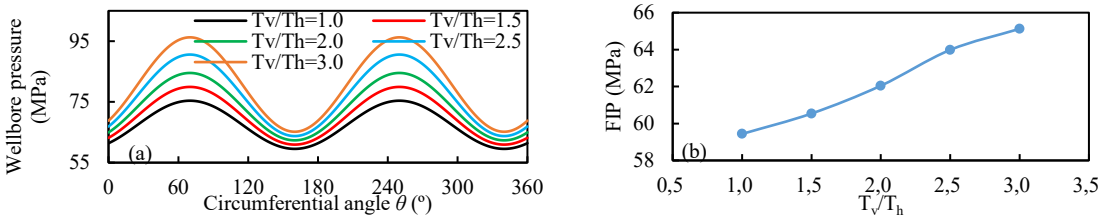

Figure 3. Distribution of wellbore pressure with angle θ (a) and variation of FIP (b) under different T_v/T_h.

3.4 *Effect of bedding dip angle*

Figure 4 shows the effect of bedding dip angle on the distribution of wellbore pressure with circumferential angle and variation of FIP. With the increase of dip angle, the crest or trough of wellbore pressure with circumferential angle gradually moves to the right and the variation of the FIP exhibits monotonously increase from 59.09MPa to 63.98MPa.

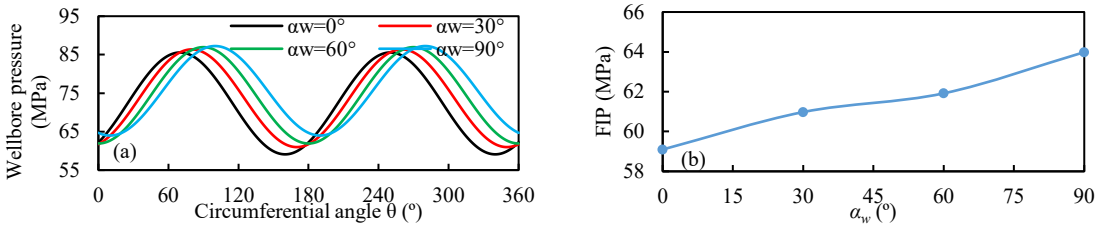

Figure 4. Distribution of wellbore pressure with angle θ (a) and variation of FIP (b) under different α_w.

3.5 *Effect of horizontal in-situ stress ratio σ_H/σ_h*

The effect of in-situ stress ratio σ_H/σ_h on the distribution of wellbore pressure with circumferential angle and variation of FIP are illustrated in Figure 5. There is a negative correlation relationship between FIP and in-situ stress ratio σ_H/σ_h. With the increase of ratio σ_H/σ_h from 1.0 to 2.0, the FIP decreases from 62.87MPa to 53.54MPa. This states that the fracture is easier to initiate under stronger anisotropy of in-situ stress.

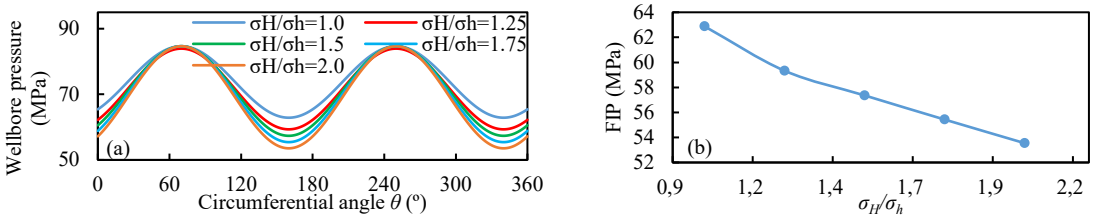

Figure 5. Distribution of wellbore pressure with angle θ (a) and variation of FIP (b) under different σ_H/σ_h.

3.6 *Effect of azimuth of horizontal well*

Figure 6 shows the distribution of wellbore pressure with circumferential angle and variation of FIP under different azimuth β of horizontal well. Here, β=0° represents that the azimuth of horizontal

well is along direction of maximum horizontal stress while β=90º represents horizontal well is along the direction of minimum horizontal stress. It is found that the FIP increases first and then decreases with the increase of azimuth of horizontal well. The maximum FIP is around 50° but the FIP along the direction of minimum horizontal stress is higher than the FIP at β=0º.

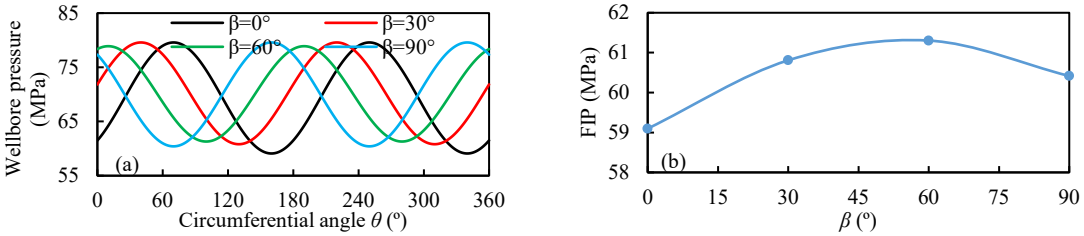

Figure 6. Distribution of wellbore pressure with angle θ (a) and variation of FIP (b) under different β.

4 CONCLUSIONS

In this work, the fracture initiation pressure (FIP) of horizontal well in transversely isotropic shale is analyzed in detail with considering both elastic modulus anisotropy and tensile strength anisotropy. Through the parametric study, in the case of $\sigma_H>\sigma_v>\sigma_h$ stress state and horizontal well along maximum horizontal stress, the increase of the anisotropy of Young's modulus, Poisson′s ratio and horizontal in-situ stress induces a reduction of the FIP. While an increase of tensile strength ratio T_v/T_h and bedding dip angle will increase the FIP. For the effect of azimuth of horizontal well, the FIP increases first and then decreases with the increase of angle between horizontal well and maximum horizontal stress. In the above parameters, the influence of E_h/E_v is the highest, followed by σ_H/σ_h, and then T_v/T_h, while the influence of Poisson's ratio is the lowest. This indicates that the anisotropic elastic properties, in-situ stresses, anisotropic tensile strength as well as bedding dip angle need to be considered comprehensively for improving the prediction accuracy of FIP.

REFERENCES

Aadnoy, B.S. 1989. Stresses around horizontal boreholes drilled in sedimentary rocks. *Journal of Petroleum Science and Engineering*, 2, pp.349-360.

Do., D.P., Tranb, N.H., Hoxhaa, D. & Dang, H.L. 2017. Assessment of the influence of hydraulic and mechanical anisotropy on the fracture initiation pressure in permeable rocks using a complex potential approach. *International Journal of Rock Mechanics and Mining Sciences*, 100, pp.108-123.

Guo, F., Morgenstern, N.R. & Scott, J.D. 1993. Interpretation of hydraulic fracturing breakdown pressure. *International Journal of Rock Mechanics and Mining Sciences & Geomechanics Abstracts*, 30(6), pp.617-626, from https://doi.org/10.1016/0148-9062(93)91221-4.

Gupta, D. & Zaman, M. 1999. Stability of boreholes in a geologic medium including the effects of anisotropy. *Applied Mathematics and Mechanics*, 20(8), pp.837-866.

Li, Y.W. & Jia, D. 2018. Fracture initiation model of shale fracturing based on effective stress theory of porous media. *Geofluids*, Article ID 2053159, pp.1-12, from https://doi.org/10.1155/2018/2053159.

Ma, T.S., Zhang, Q.B., Chen, P., Yang, C.H. & Zhao, J. 2017. Fracture pressure model for inclined wells in layered formations with anisotropic rock strengths. *Journal of Petroleum Science and Engineering*, 149, pp.393-408.

Ma, T.S, Liu, Y. & Chen, P. 2019. Fracture-initiation pressure analysis of horizontal well in anisotropic formations. *International Journal of Oil, Gas and Coal Technology*, 22(4), pp.447-469.

Ma, T.S., Wang, H.N., Liu, Y., Shi, Y.F. & Ranjith, P.G. 2022. Fracture-initiation pressure model of inclined wells in transversely isotropic formation with anisotropic tensile strength. *International Journal of Rock Mechanics & Mining Sciences*, 159, 105235.

Ong, S.H. & Roegiers, J.C. 1995. Fracture initiation from inclined wellbores in anisotropic formations. In: *International Meeting on Petroleum Engineering*, Beijing, PR China, November 14- 17, 1995, SPE29993.

Sampath, K.H.S.M., Perera, M.S.A. & Ranjith, P.G. 2018. Theoretical overview of hydraulic fracturing break-down pressure. Journal of Natural Gas Science and Engineering, 58, pp.251-265.

Zhang, J.C. & Yin, S.X. 2017. Fracture gradient prediction: an overview and an improved method. *Petroleum Science*, 14, pp.720-730.

Zhao, K., Yuan, J.L., Feng, Y.C. & Yan, C.L. 2018. A novel evaluation on fracture pressure in depleted shale gas reservoir. *Energy Science & Engineering*, 6(3), pp.201-216.